An Electron Paramagnetic Resonance Study of $Mn_2(H_2O)(OAc)_4(tmeda)_2$ (tmeda = *N,N,N′,N′*-Tetramethylethylenediamine): A Model for Dinuclear Manganese Enzyme Active Sites

Timothy Howard,[†] Joshua Telser,[‡] and Victoria J. DeRose*[,†]

Department of Chemistry, Texas A&M University, College Station, Texas 77842-3012, and Chemistry Program, Roosevelt University, Chicago, Illinois 60605-1394

Received January 5, 2000

The complex $Mn_2(H_2O)(OAc)_4(tmeda)_2$ (tmeda = *N,N,N′,N′*-tetramethylethylenediamine) is a model for the active site of hydrolase enzymes containing acetate-bridged dimanganese cores. The two high-spin Mn(II) ions are antiferromagnetically coupled, as determined by previous magnetic susceptibility studies (Yu, S.-B; Lippard, S. J.; Shweky, I; Bino, A. *Inorg. Chem.* **1992**, *31*, 3502−3504) to yield a spin "ladder" with total spin $S = 0, 1, 2, ..., 5$ in increasing energy. In this study, the complex was characterized by Q-band and X-band EPR spectroscopy in frozen solution. Analysis of the temperature dependence of these EPR spectra indicates that the primary spectral contribution is from the $S = 2$ manifold. The EPR spectra were simulated using a full spin Hamiltonian for this manifold of a coupled spin system, which provided the fit parameters $J = -2.9$ cm^{-1}, $g = 2.00$, and $D_2 = -0.060 \pm 0.003$ cm^{-1}. An additional multiline EPR signal is observed which is proposed to arise from the total spin $S = 5/2$ ground state of a Mn(II) trimer of the type $Mn_3(OAc)_6(tmeda)_2$.

Introduction

Several enzymes contain a dimanganese(II,II) center, including arginase, catalase, thiosulfate-oxidizing enzyme, and a glycohydrolase.[1−4] Another group of enzymes have a Mg^{2+} or Zn^{2+} binuclear metal center in the native state but retain some activity when substituted with Mn(II); these include ribonuclease H, phosphotriesterase, enolase, and *S*-adenosylmethionine synthetase.[5−8] In nearly all of the dimanganese and binuclear metal-containing enzymes for which structures are known, the metals are bridged by at least one glutamate or aspartate residue and often a water or hydroxide group. These observations have motivated the synthesis and characterization of several dimanganese(II,II) model compounds with bridging acetate and aquo ligands.[9−15]

The two Mn(II) ions (high-spin $3d^5$, $S_1 = S_2 = 5/2$) in these proteins and model compounds experience weak antiferromagnetic exchange coupling ($\mathbf{H} = -2JS_1 \cdot S_2$),[16] which leads to a "ladder" of spin states, with total spin $S = 0, 1, 2, 3, 4$, and 5 in order of increasing energy. This coupled spin system gives rise to complex EPR spectra that can contain features from multiple spin states with temperature-dependent populations. The EPR spectra are further complicated by the effect of hyperfine coupling to ^{55}Mn ($I = 5/2$, 100% natural abundance). An understanding of the relation between structural and EPR properties in model compounds should aid in obtaining such information from EPR spectra of structurally uncharacterized protein systems. The complexity of the exchange-coupled $^{55}Mn_2$ spin system has, however, made full simulations of spectra from these centers difficult. Khangulov et al.[17] have developed a procedure based on spectral deconvolution that allows estimation of the zero-field splitting parameters within the total spin $S = 2$ manifold of a dimanganese(II,II) complex. A linear correlation was found between the zero-field values and known Mn−Mn distances of several compounds. This correlation allowed the estimation of the internuclear distance for dinuclear manganese compounds once their zero-field splitting was determined. Results of this procedure were

* Corresponding author. Phone: (979) 862-1401. Fax: (979) 845-4719. E-mail: derose@mail.chem.tamu.edu.
[†] Texas A&M University.
[‡] Roosevelt University.

(1) Reczkowski, R. S.; Ash, D. E. *J. Am. Chem. Soc.* **1992**, *114*, 10992−10994.
(2) Khangulov, S. V.; Barynin, V. V.; Voevodskaya N. V.; Grebenko, A. I. *Biochim. Biophys. Acta* **1990**, *1020*, 305−310.
(3) Cammack, R.; Chapmann, A.; Lu, W.-P.; Karagouni, A. A.; Kelly, D. P. *FEBS Lett.* **1989**, *253*, 239−243.
(4) Antharavally, B. S.; Poyner, R. R.; Ludden, P. W. *J. Am. Chem. Soc.* **1998**, *120*, 8897−8898.
(5) Cirino, N. M.; Cameron, C. E.; Smith, J. S.; Rausch, J. W.; Roth, M. J.; Benkovic, S. J.; Le Grice, S. F. J. *Biochemistry* **1995**, *34*, 9936−9943.
(6) Chae, M. Y.; Omburo, G. A.; Lindahl, P. A.; Raushel, F. M. *J. Am. Chem. Soc.* **1993**, *115*, 12173−12174.
(7) Chien, J. C. W.; Westhead, E. W. *Biochemistry* **1971**, *10*, 3198−3203.
(8) Markham, G. D. *J. Biol. Chem.* **1981**, *256*, 1903−1914.
(9) Wieghardt, K.; Bossek, U.; Bonvoisin, J.; Beauvillain, P.; Girerd, J. J. *Angew. Chem., Int. Ed. Engl.* **1986**, *98*, 1026−1027.
(10) Yu, S. −B.; Lippard, S. J.; Shweky, I.; Bino, A. *Inorg. Chem.* **1992**, *31*, 3502−3504.
(11) Weighardt, K.; Bossek, U.; Nuber, B.; Weiss, J.; Bonvoisin, J.; Corbella, M.; Vitols, S. E.; Girerd, J. J. *J. Am. Chem. Soc.* **1988**, *110*, 7398−7411.
(12) Suzuki, M.; Mikuriya, M.; Murata, S.; Uehara, A.; Oshio, H.; Kida, S.; Saito, K. *Bull. Chem. Soc. Jpn.* **1987**, *60*, 4305−4312.
(13) Gultneh, Y.; Farooq, A.; Liu, S.; Karlin, K. D.; Zubieta, J. *Inorg. Chem.* **1992**, *31*, 3607−3611.
(14) Caneschi, A.; Ferraro, F.; Gatteschi, D.; Melandri, M. C.; Rey, P.; Sessoli, R. *Angew. Chem., Int. Ed. Engl.* **1989**, *28*, 1365−1368.
(15) Sakiyama, H.; Tamaki, H.; Kodera, M.; Matsumoto, N.; Okawa, H. *J. Chem. Soc., Dalton Trans.* **1993**, 591−595.
(16) The exchange coupling parameter, *J*, is sometimes defined instead as $\mathbf{H} = JS_1 \cdot S_2$. The program DDPOWJHE in fact uses the $\mathbf{H} = JS_1 \cdot S_2$ formalism; however, all *J* values reported in this paper are based on the definition $\mathbf{H} = -2JS_1 \cdot S_2$ to provide an easy comparison among exchange couplings given in previous studies.
(17) Khangulov, S. V.; Pessiki, P. J.; Barynin, V. V.; Ash, D. E.; Dismukes, G. C. *Biochemistry* **1995**, *34*, 2015−2025.

10.1021/ic0000247 CCC: $19.00
Published on Web 07/01/2000

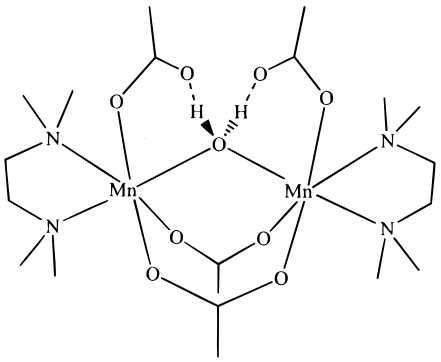

Figure 1. Structure of $Mn_2(H_2O)(OAc)_4(tmeda)_2$ (**1**). Adapted from ref 10. Copyright 1992 American Chemical Society.

presented for catalase, arginase, and a series of model compounds. Recently, Chan and co-workers[18] have recorded and simulated the EPR signal from the compound $Mn_2(OAc)_4(imidazole)_4(H_2O)$[19] in the solid state. No resolved hyperfine coupling was observed in the EPR spectrum, and the spectral breadth was simulated using a line-broadening function.

To understand these centers further, we have sought a full simulation of the X- and Q-band spectra of an appropriate model compound. The X-ray crystal structures and magnetic susceptibility data of two such model compounds, $Mn_2(H_2O)(pivalate)_4(Me_2bpy)_2$ and $Mn_2(H_2O)(OAc)_4(tmeda)_2$ (tmeda = *N*,*N*,*N*′,*N*′-tetramethylethylenediamine), have been reported by Yu et al.[10] EPR data were not reported for these compounds. We have synthesized $Mn_2(H_2O)(OAc)_4(tmeda)_2$ and obtained its EPR signals in a frozen solution. The EPR spectra of $Mn_2(H_2O)(OAc)_4(tmeda)_2$ dissolved in toluene are consistent with an exchange-coupled dinuclear manganese center. These frozen solutions give well-resolved EPR spectra, and in the noncoordinating, aprotic toluene solvent, it is likely that the solid-state structure is generally maintained. These factors make this complex a good target for a detailed EPR analysis.

The frozen solution EPR spectra of $Mn_2(H_2O)(OAc)_4(tmeda)_2$ at both Q-band (35 GHz) and X-band (9 GHz) microwave frequencies are reported here, and the concentration dependence and temperature dependence of the spectra are investigated. We show that the resolved lines in the EPR spectra are due to transitions within the total spin $S = 2$ state of this exchange-coupled system. These EPR spectra are simulated using the full spin Hamiltonian for such an exchange-coupled system, from which the zero-field splitting within the $S = 2$ manifold was determined to be $D_2 = -0.060 \pm 0.003$ cm^{-1}. An additional signal observed in the Q-band spectra with a g value near 4.52 and with resolved hyperfine lines with a splitting of 26 G is proposed to arise from a Mn(II) trimer.

Experimental Section

Materials. $Mn_2(H_2O)(OAc)_4(tmeda)_2$ (**1**; Figure 1) was synthesized as reported previously.[10] In brief, $Mn(OAc)_2{\cdot}4H_2O$ (1.0 g, 0.41 mmol) was dissolved in degassed methanol (50 mL), and tmeda (0.62 mL, 0.41 mmol) was added under nitrogen. The mixture was stirred for 10 min, and then the methanol was removed in vacuo, leaving a solid residue. The residue was extracted with 30 mL of hexane, filtered, and then recrystallized from the hexane solution by cooling to −20 °C.

Methods. Q-band EPR measurements were carried out on a modified Bruker ESP-200 spectrometer equipped with a Varian E-110 microwave bridge operating at 34 GHz[20] and a cylindrical cavity[21] inside a Janis 7.5 CNDT-SVT liquid helium dewar. The temperature in the liquid helium dewar was recorded with a sensor attached to the top of the cavity and controlled with a LTC-10 temperature controller from Conductus.

X-band EPR measurements were performed on a Bruker ESP-300 instrument with a rectangular TE_{102} cavity and an Oxford cryostat.

Solutions of $Mn_2(H_2O)(OAc)_4(tmeda)_2$ in polar solvents such as acetone were found to give EPR signals consistent with mononuclear compounds. However, $Mn_2(H_2O)(OAc)_4(tmeda)_2$ also proved to be soluble in weakly or noncoordinating solvents such as toluene, dichloromethane, and THF. The EPR spectra of $Mn_2(H_2O)(OAc)_4(tmeda)_2$ dissolved in these solvents were consistent with an exchange-coupled dinuclear manganese center.

EPR spectra were simulated with a FORTRAN 99 computer program, DDPOWJHE, running on a Cray J90 computer, which employs the full spin Hamiltonian for an exchange-coupled two-spin system.[22] The spin Hamiltonian is

$$\mathbf{H} = -2JS_1{\cdot}S_2 + S_1{\cdot}\mathbf{D}{\cdot}S_2 + \sum_{i=1}^{2}(S_i{\cdot}\boldsymbol{D}_i{\cdot}S_i + \beta B{\cdot}\boldsymbol{g}_i{\cdot}S_i + \beta_n g_n B{\cdot}I_i + S_i{\cdot}\mathbf{A}_i{\cdot}I_i) \quad (1)$$

where the terms correspond to isotropic exchange coupling, dipolar exchange coupling, single-ion zero-field splitting, electronic and nuclear Zeeman splitting, and hyperfine coupling, respectively. All the terms in eq 1 are included in the Hamiltonian matrix. Matrix diagonalization using LAPACK subroutines yields the eigenvalues and eigenvectors, from which the EPR transition energies and probabilities, respectively, are determined. The program contains a temperature-dependent Boltzmann weighting factor, a general line-broadening feature, and the ability to select the specific transitions being simulated. The program uses the igloo method to calculate the powder pattern. Full powder pattern spectra were simulated using igloo = 100 and a large line-broadening function with no hyperfine included. Spectra including the hyperfine interaction were calculated at only the principal axes (igloo = 1) to reduce the computational time.

The full Hamiltonian for a coupled S_1, $S_2 = 5/2$, I_1, $I_2 = 5/2$ system leads to a 1296 × 1296 matrix. Since the major signals observed in the EPR spectra were due to the $S = 2$ state (i.e., the higher energy coupled spin states with $S = 3$, 4, and 5 do not contribute to the observed low-temperature spectra), the Hamiltonian in those simulations was therefore simplified to a coupled S_1, $S_2 = 1$, I_1, $I_2 = 5/2$ system. This leads to a 324 × 324 matrix, which significantly reduces the computational time. EPR transitions are thus determined for the resulting $S = 2$ coupled spin state, which includes the zero-field splitting term D_2. The zero-field splitting was included as one parameter for the $S = 2$ state, D_2, although the program does allow the separate entry of the single-ion zero-field splitting value D_c and the dipolar coupling D_d. Estimation of these values is described in the Discussion. The error in D_2 was estimated from the change in D_2 necessary to produce a noticeable change in the fit of the simulated spectrum to the experimental spectrum. The source code is available from the authors.

The Boltzmann populations of the total spin $S = 1$ and $S = 2$ levels within an exchange-coupled $S_1 = S_2 = 5/2$ system with an exchange coupling constant of $J = -2.9$ cm^{-1} were calculated on the basis of eq 2. The signal intensity of the EPR signals was determined by averaging the peak heights of the three most intense peaks for each 11-line pattern and multiplying by the temperature to remove the Curie dependence of the spectra.

Electrospray ionization mass spectra were acquired using a Vestec-200 mass spectrometer operating in negative ion mode. Solutions for

(18) Schultz, B. E.; Ye, B.-H.; Li, X.-y; Chan, S. I. *Inorg. Chem.* **1997**, *36*, 2617−2622.

(19) Abbreviations: OAc, acetate; Me_2bpy, 4,4′-dimethyl-2,2′-bipyridine; bpy, bipyridine; tmeda, *N*,*N*,*N*′,*N*′-tetramethylethylenediamine; ESI, electrospray ionization mass spectrometry.

(20) Morrissey, S. R.; Horton, T. E.; DeRose, V. J. *J. Am. Chem. Soc.* **2000**, *122*, 3473−3481.

(21) Sienkiewicz, A.; Smith, B. G.; Veselov, A.; Scholes, C. R. *Rev. Sci. Instum.* **1996**, *67*, 2134−2138.

(22) Howard, T.; Vellas, S.; DeRose, V. J.; Telser. J. *J. Magn. Reson.*, manuscript in preparation.

use in the ESI spectrometer were prepared by dissolving $Mn_2(H_2O)(OAc)_4(tmeda)_2$ in dichloromethane.

$$\text{population}_s = \frac{(2S+1)\exp([-2J(S(S+1)-S_1(S_1+1)-S_2(S_2+1))]/kT)}{\sum_s (2S+1)\exp([-2J(S(S+1)-S_1(S_1+1)-S_2(S_2+1))]/kT)} \quad (2)$$

Results

The variable-temperature Q-band EPR spectra near $g = 2$ of a 16 mM toluene solution of $Mn_2(H_2O)(OAc)_4(tmeda)_2$ are shown in Figure 2. Two sets of eleven lines split by 45 G and centered at $g = 2.00$ are observed in all spectra over the range 6−50 K. This 11-line pattern ($2nI + 1 = 4(5/2) + 1 = 11$) indicates a coupled manganese system, consistent with the magnetic susceptibility results reported for this compound in the solid state.[10] The intensity of the observed lines reaches a maximum at 17 K. A second set of two transitions with resolved hyperfine splitting at much lower intensity can also be observed centered at $g = 1.89$ and $g \approx 2.08$.

X-band spectra of **1** in toluene solution were obtained over the temperature range 5−50 K (Figure 3). These spectra show two sets of eleven lines, each separated by 45 G, that are similar to the Q-band spectrum, but centered at $g \approx 2.14$. A set of lines separated by 45 G with much lower intensity are centered near $g = 2.52$. Several additional features can be observed in the X-band spectrum including ones at $g = 1.60$, $g = 2.6$, $g = 3.36$, $g = 4.36$, and $g = 13.9$.

The full-width Q-band spectrum in toluene solution is shown in Figure 4. In addition to the hyperfine split features centered near $g = 2$, a derivative feature at $g = 4.52$ is observed that increases in intensity as the temperature is lowered (Figure S1 in the Supporting Information). In dichloromethane solution at low concentrations, more than 25 lines with hyperfine splitting of 26 G can be observed on the $g = 4.52$ peak (Figure 4). The position and symmetric line shape of the signal observed at $g = 4.52$ suggest that it arises from a transition involving a total spin $S = 5/2$ state.[23] One possible source of an $S = 5/2$ signal would be formation of a trinuclear Mn(II) species.[24] No large derivative feature at $g = 4.52$ was observed in the X-band spectra, in contrast to the Q-band spectra.

Evidence for yet another, EPR-silent, species in solution is found in Q-band EPR spectra showing the effects of diluting a concentrated 102 mM solution of $Mn_2(H_2O)(OAc)_4(tmeda)_2$ (Figure S2). When the stock solution is diluted by half, the signal intensity of the $g = 4.52$ peak, the $g = 2.12$ feature, and the peaks attributed to the dimer decrease by a factor of roughly 2. When the stock solution was diluted by a factor of 3, however, all the peak intensities decreased by more than a factor of 3 and the line shape at $g = 2$ changed, indicating possible equilibrium with another complex which is EPR silent, such as a compound with a much larger J, or that the compound has been oxidized to a Mn(III) complex.

Discussion

When the isotropic exchange coupling constant J has larger magnitude than both the Zeeman and the zero-field splitting

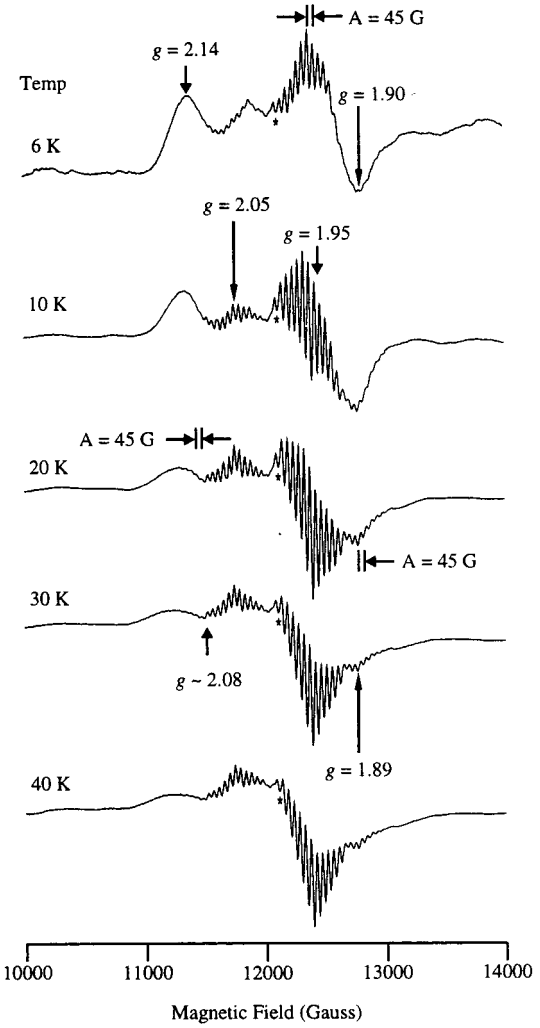

Figure 2. Variable-temperature Q-band spectra of **1** [16 mM, toluene]. EPR conditions: 33.8 GHz spectrometer frequency, 1.17 mW microwave power, 0.59 G modulation amplitude, 100 kHz modulation frequency. The small peak marked with an asterisk occurs in the Q-band spectra at $g = 1.99$, which is very close to the set of peaks at $g = 1.95$. It is split from the nearest peaks by 52 G instead of 45 G. Its identity is unknown.

for a dimanganese system, then the energy levels in an external magnetic field **B** are given by solving the Hamiltonian[25]

$$\mathbf{H} = -2J[(S(S+1) - S_1(S_1+1) - S_2(S_2+1)] + \beta\mathbf{B}\cdot\mathbf{g}\cdot\mathbf{S} + D_S[S_z^2 - 1/3(S(S+1)] + E_S(S_x^2 - S_y^2) + \mathbf{S}\cdot\mathbf{A}\cdot(\mathbf{I}_1 + \mathbf{I}_2) \quad (3)$$

where S is the system total spin given by $S = |S_1 + S_2|, |S_1 + S_2 - 1|, ..., |S_1 - S_2|$ and D_S and E_S are the zero-field splitting for the exchange-coupled pair. The zero-field splitting term D_S is a sum of two components:

$$D_S = 3\alpha_s D_e + \beta_s D_c \quad (4)$$

where for $S_1 = S_2 = 5/2$

$$\alpha_s = (1/2)[S(S+1) + 35]/[(2S-1)(2S+3)] \quad (5)$$

$$\beta_s = [3S(S+1) - 38]/[(2S-1)(2S+3)] \quad (6)$$

where D_c is the single-ion zero-field splitting and D_e is the zero-field splitting arising from the coupling of the spins. The zero-

(23) Haddy, A.; Dunham, W. R.; Sands, R. H.; Aasa, R. *Biochim. Biophys. Acta* **1992**, *1099*, 25−34.
(24) Ménage, S.; Vitols, S. E.; Bergerat, P.; Codjovi, E.; Kahn, O.; Girerd, J.-J.; Guillot, M.; Solans, X.; Calvet, T. *Inorg. Chem.* **1991**, *30*, 2666−2671.

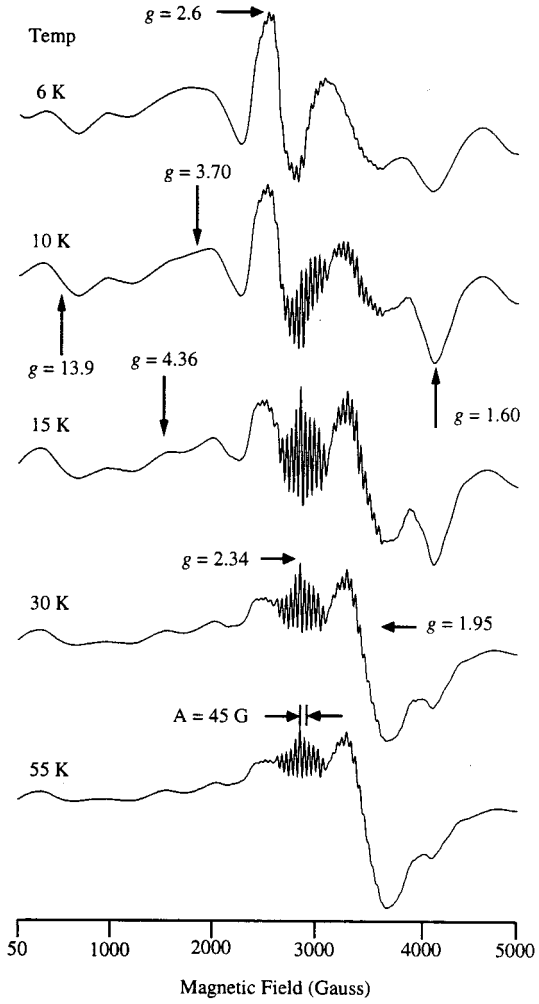

Figure 3. Variable-temperature X-band spectra of **1** [16 mM, toluene]. EPR conditions: 9.42 GHz spectrometer frequency, 2 mW microwave power, 14.6 G modulation amplitude, 100 kHz modulation frequency.

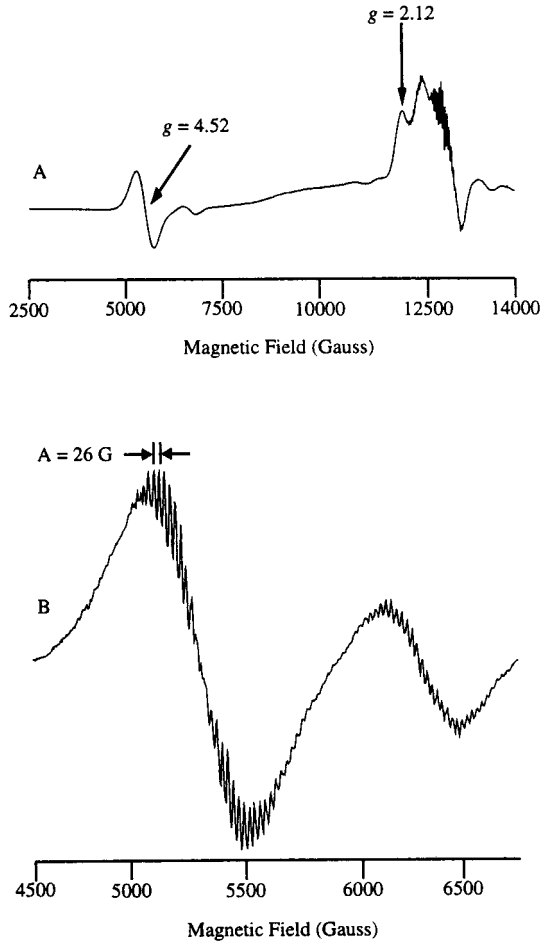

Figure 4. (A) Q-band spectra of **1** [16 mM, toluene]. EPR conditions: 33.8 GHz spectrometer frequency, 1.17 mW microwave power, 0.59 G modulation amplitude, 100 kHz modulation frequency, temperature 7 K. (B) Low-field region of the Q-band spectra of **1** [25 mM, dichloromethane, temperature 4 K]. EPR conditions: 33.8 GHz spectrometer frequency, 1.17 mW microwave power, 0.59 G modulation amplitude, 100 kHz modulation frequency.

field splitting imposed by the coupling, D_e, in turn has two contributions:[26,27]

$$D_e = D_d + D_E = -3g^2\beta^2/2r^3 + D_E \qquad (7)$$

where D_d is the direct dipolar coupling interaction, which depends on the distance, r, between the two spins and D_E is the pseudodipolar exchange. The pseudodipolar term is usually considered to be negligible[28] if $|J| < 60$ cm^{-1}, which is clearly the case here, so that D_e depends mainly on the spin−spin separation.

Spin−spin coupling between two Mn(II) ions leads to several characteristic EPR features. The EPR spectra of coupled dinuclear centers arise from within a ladder of spin states that are separated in energy by multiples of the spin exchange term J. For dinuclear Mn(II) centers the spin states available are $S = 0-5$. In most acetate-bridged dinuclear Mn(II) complexes, J has sufficiently small magnitude that several different spin states may be populated simultaneously in the range 10−20 K, which leads to a large number of observed EPR transitions. For a symmetric exchange-coupled pair, the number of observed hyperfine lines increases from six to eleven (for an isotropic spectrum) and the observed hyperfine splitting is roughly half the value expected for the individual ions (45 G versus 90 G).[29]

The exchange coupling constant J can be determined by variable-temperature magnetic susceptibility measurements or by variable-temperature EPR intensity measurements, in either case by fitting the data to the calculated J-dependent Boltzmann populations. The coupling constant for **1** has already been determined by magnetic susceptibility to be $J = -2.9$ cm^{-1}.[10] We therefore compared the temperature dependence of the hyperfine resolved Q-band EPR signals at $g = 2.05$ and $g = 1.95$ to the Boltzmann populations expected for the $S = 0$, $S = 1$, and $S = 2$ spin states, in an attempt to determine from which level(s) the signals originate (Figure 5). The increase in signal intensity over the temperature range 6−20 K for both sets of well-resolved peaks matches the increase in Boltzmann population expected for the $S = 2$ level, while a fit to intensities expected for an $S = 1$ state are unsuccessful. From this we conclude that the $g = 2$ EPR signal with resolved hyperfine splitting originates predominantly from the $S = 2$ state.

The main features of the spectra were simulated by a program that uses a full spin Hamiltonian treatment of the exchange

(25) Owen, J. *J. Appl. Phys.* **1961**, *32*, 213S−215S.
(26) Pilbrow, J. R. *Transition Ion Electron Paramagnetic Resonance*; Oxford Science Publications: New York, 1990; pp 360.
(27) Eaton, S. S.; More, K. M.; Sawant. B. M.; Eaton, G. R. *J. Am. Chem. Soc.* **1983**, *105*, 6560−6567.
(28) Smith, T. D.; Pilbrow, J. R. *Coord. Chem. Rev.* **1974**, *13*, 173−278.
(29) Reed, G. H.; Markham, G. D. *Biological Magnetic Resonance Volume 6*; Plenum Press: New York, 1984; pp 73−135.

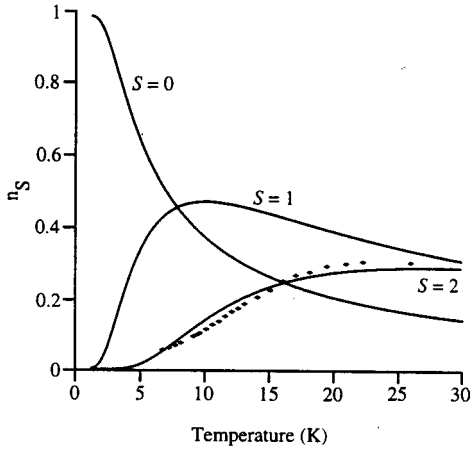

Figure 5. Comparison of the temperature variation of hyperfine peaks in the Q-band EPR signal of **1** (diamonds) to the expected population of the $S = 0$, $S = 1$, and $S = 2$ states (solid lines) calculated from an exchange coupling of $J = -2.9$ cm^{-1} (eq 2). Experimental data are plotted as normalized EPR signal amplitude vs temperature (K).

coupling, Zeeman, zero-field splitting, and hyperfine terms. As discussed above, the resolved features are thought to be EPR transitions within the total spin $S = 2$; thus, calculations involving transitions within manifolds with $S > 2$ are ignored. For these calculations, it was assumed that g is isotropic, A is isotropic, $J = -2.9$ cm^{-1} as determined by magnetic susceptibility,[10] and the zero-field splitting is axially symmetric ($E_2 = 0$). A comparison of the Q-band spectrum to a simulation including hyperfine interactions and a simulation without hyperfine interactions is shown in Figure 6, and a simulation of the X-band spectrum is shown in Figure 7. Simulations without hyperfine interactions were calculated to yield the full powder pattern, which matches the overall broad line shape of the experimental spectra. As described below, the hyperfine patterns of the experimental spectra appear to arise from a subset of transitions, and these patterns are matched by simulations including hyperfine that were calculated at the principal axes.

These simulations give insight into the origin of the main features in the experimental EPR spectra. Four allowed $\Delta M_S = 1$ transitions are expected within the $S = 2$ manifold along one direction of the magnetic field molecular axis (Figure 8). For an axial system, a powder pattern with eight total turning points is expected. The two well-resolved features in the experimental spectra near $g = 2$ represent two of the four expected perpendicular transitions. These are labeled XY_2 and XY_3 and correspond to $\Delta M_S = 1$ transitions between $M_S = +1$, -1 and $M_S = 0$. The two transitions with resolved hyperfine splitting and much lower signal intensity are assigned to the corresponding parallel transitions Z_2 and Z_3 (Figure 8). Two broad features in the experimental spectrum appear at the calculated position of the two other perpendicular transitions XY_1 and XY_4 which are due to $\Delta M_S = 1$ transitions between $M_S = +2$, -2 and $M_S = +1$, -1. These features do not show any resolved hyperfine structure in the experimental spectrum. For systems in which $D \ll g\beta B$ the transition frequencies of all four transitions are given by[30]

$$h\nu/g\beta \pm u/2g\beta \ (M_S = +1, -1 \rightarrow 0;\ Z/XY_2,\ Z/XY_3) \quad (8)$$

$$h\nu/g\beta \pm 3u/2g\beta \ (M_S = +2, -2 \rightarrow +1, -1;\ Z/XY_1,\ Z/XY_4) \quad (9)$$

where $u = D(3\cos^2\theta - 1) + 3E(\cos 2\phi \sin^2\theta)$. Given that the XY_1 and XY_4 transitions have a 3-fold greater dependence

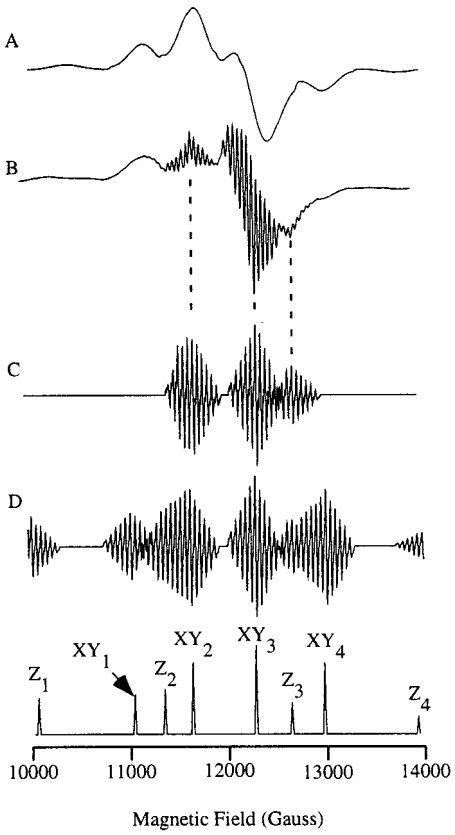

Figure 6. Comparison of the Q-band EPR signals of **1** to a simulation of the $S = 2$ state of a coupled Mn(II) system: (A) simulation of the $S = 2$ states with $g = 2.01$, $A(^{55}Mn) = 0$, $D_2 = -0.053$ cm^{-1}, and line width 400 MHz, full powder pattern; (B) 16 mM in toluene with EPR conditions 33.83 GHz spectrometer frequency, 1.17 mW microwave power, 0.59 G modulation amplitude, 100 kHz modulation frequency, and temperature 15 K; (C) simulation including only the XY_2, XY_3, and Z_3 transitions of the $S = 2$ state with $g = 2.00$, $A(^{55}Mn) = 272$ MHz, $D_2 = -0.060$ cm^{-1}, and Gaussian line width 40 MHz, principal axes only; (D) simulation of the $S = 2$ state, with parameters as in (C), principal axes only.

on the zero-field splitting value than the transitions XY_2 and XY_3, a small amount of D strain (i.e., a distribution in D values arising from structural disorder) could have the effect of broadening the outer transitions proportionally much more than the inner transitions.

D strain could also explain the failure to observe hyperfine split signals arising from transitions within the total spin $S = 1$ manifold. Simulations of the $S = 1$ state show that the broad transitions that increase in intensity below 15 K at $g = 3.70$ and $g = 1.60$ in the X-band spectrum and $g = 2.14$ and $g = 1.90$ in the Q-band spectrum probably should be assigned to the $S = 1$ state of the coupled system (Figure S3). The zero-field splitting of the $S = 1$ level is 3.7 times that of the $S = 2$ level due to the dependence of the zero-field splitting on S as shown in eqs 4−6, and would thus be expected to be proportionally affected by D strain more than the transitions in the $S = 2$ manifold. We currently have no way to reproduce this D strain in the simulations, but Figures 6A and 7A show simulations in which this effect is modeled for the $S = 2$ state simply by increasing the spectral line width. It can be seen that a Gaussian line width of 400 MHz reproduces well the outer (XY_1 and XY_4) transitions, while a line width of only 40 MHz

(30) Weltner, W. *Magnetic Atoms and Molecules*; Dover Publications Inc.: New York, 1983; pp 256−265.

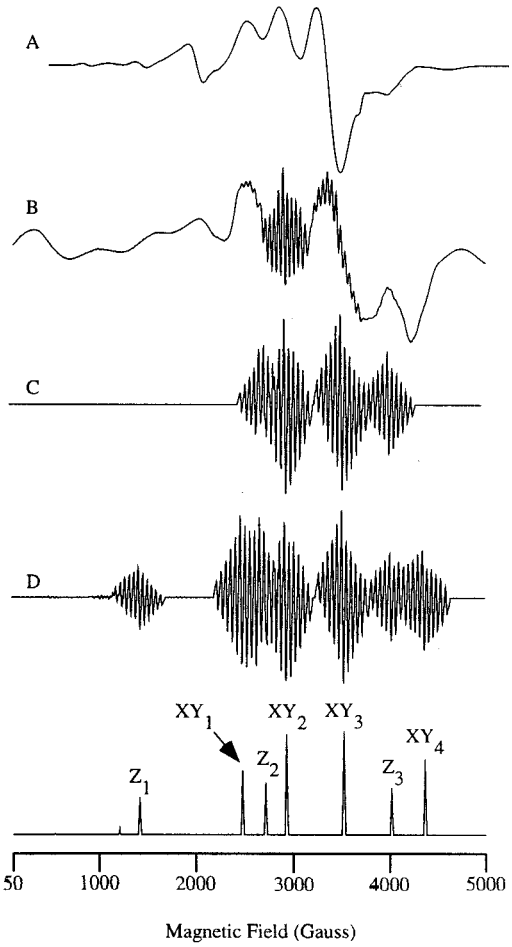

Figure 7. Comparison of the X-band EPR signals of **1** to a simulation of the $S = 2$ state of a coupled Mn(II) system: (A) simulation of the $S = 2$ states with $g = 2.01$, $A = 0$, $D_2 = -0.053$ cm^{-1}, and line width 400 MHz, full powder pattern; (B) 16 mM in toluene with EPR conditions 9.42 GHz spectrometer frequency, 2 mW microwave power, 14.6 G modulation amplitude, 100 kHz modulation frequency, temperature 15 K; (C) simulation including only the Z_2, XY_2, XY_3, and Z_3 transitions of the $S = 2$ state with $g = 2.00$, $A(^{55}\text{Mn}) = 272$ MHz, $D_2 = -0.060$ cm^{-1}, and Gaussian line width 40 MHz, principal axes only; (D) simulation of the $S = 2$ state, with the parameters as in (C), principal axes only.

reproduces the inner (XY_2 and XY_3) transitions with their resolved hyperfine splitting (Figures 6C and 7C).

Good fits to the hyperfine splittings of the experimental Q-band and X-band spectra are produced using a zero-field splitting of the $S = 2$ level of $D_2 = -0.060 \pm 0.003$ cm^{-1}. This value is determined to within 30 G (0.0030 cm^{-1}) by matching the centers of the simulated 11-line hyperfine patterns from XY_2 and XY_3 to the experimental spectra, in particular for the Q-band spectra of Figure 6C. Calculation of the dipolar coupling with eq 7 using the crystallographically determined Mn−Mn distance of 3.62 Å[10] gives a value of $D_d = -0.029$ cm^{-1}. The difference between D_2 and D_d ($\sim$0.03 cm^{-1}) is due to the contribution from single-ion zero-field splitting, D_c, in eq 4. D_c values in the range 0−0.05 cm^{-1} have been reported for mononuclear Mn(II).[31] Dismukes and co-workers[17] found a linear correlation between the internuclear distance and D_2 over the distance of 3.0 to $\sim$4 Å, and the value obtained here agrees well with their dataset. As they point out, lacking independent information regarding D_c, it would not be possible to use D_d to extract a distance in an unknown compound. A better fit to the broad peaks in the Q-band and X-band spectra is obtained when the zero-field splitting is reduced to $D_2 = -0.053 \pm 0.002$ cm^{-1} (Figures 6A and 7A). Simulations of the hyperfine split lines with $D_2 = -0.053 \pm 0.002$ cm^{-1} did not, however, produce a satisfactory fit to the experimental spectrum. This discrepancy might be related to modeling D strain in the simulation.

(31) Misra, S. K. *Physica B* **1994**, *203*, 193−200 and references therein.

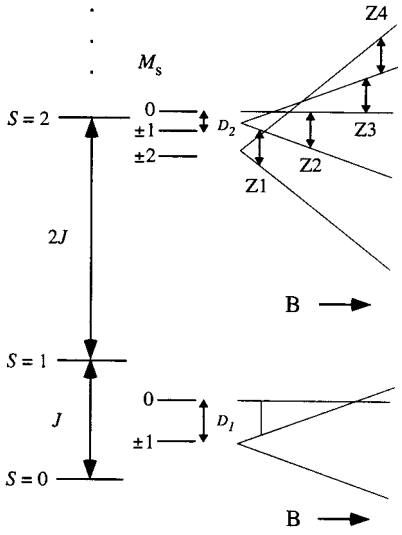

Figure 8. Diagram showing the spin ladder caused by exchange coupling between two equivalent Mn(II) $S = 5/2$ ions. The Zeeman levels at the four $\Delta M_S = 1$ parallel transitions for the $S = 2$ level of the coupled manganese cluster assuming $D < 0$ are shown (21-24).

Also of interest is the observation of a symmetric peak at $g = 4.52$ for **1** in the Q-band measurements in dichloromethane and toluene solutions. The peak grows in intensity as the temperature is lowered to $\sim$4 K, which suggests that the signal comes from a ground state or a very low lying excited state. The observation of a 26 G hyperfine splitting possibly rules it out as belonging to a $\Delta M_S = 2$ (formally forbidden) transition, since the hyperfine splitting of the $\Delta M_S = 2$ transition should be the same as the allowed $\Delta M_S = 1$ transition as long as the radius between the coupled spins is less than $\sim$4.5 Å,[27] which is the case here. The S_2 state of the oxygen-evolving complex from spinach, in oriented samples, exhibits a signal at $g = 4.1$ with at least 16 resolved hyperfine lines separated by 36 G.[32] Haddy and co-workers[23] attributed this signal to a total spin 5/2 system on the basis of simulations of spectra obtained at multiple frequencies.

A possible explanation for the observation of this signal in frozen solutions of **1** is that a trinuclear complex of the type $(Mn(II))_3$ is formed. The hyperfine splitting of such a system (if symmetric) should be $A/3$ or $\sim$30 G, similar to the observed value of 26 G. A dinuclear manganese(II) acetate complex, analogous to **1**, can form a trinuclear complex, $Mn_3(OAc)_6(bipy)_2$, which was shown by magnetic susceptibility studies to have a total spin 5/2 ground state.[24] Mass spectra acquired by ESI for **1** dissolved in dichloromethane show, in addition to fragments from $Mn_2(H_2O)(OAc)_4(tmeda)_2$, a peak at 751 mass units consistent with the presence of a trinuclear cluster with the formula $Mn_3(OAc)_6(tmeda)_2$ (data not shown).

Summary

The complex $Mn_2(H_2O)(OAc)_4(tmeda)_2$ (**1**) was characterized by EPR spectroscopy in frozen solution at X- and Q-band

(32) Kim, D. H.; Britt, R. D.; Klein, M. P.; Sauer, K. *J. Am. Chem. Soc.* **1990**, *112*, 9389−9391.

microwave frequencies. Unlike many previous studies of dinuclear manganese compounds which were performed in the solid state, the frozen solution EPR spectrum of **1** exhibits resolved hyperfine features which occur as sets of 11 lines separated by 45 G. Variable-temperature data show that the primary contribution to the EPR spectra at both frequencies arises from transitions within the total spin $S = 2$ manifold. A computer program employing the full spin Hamiltonian for an exchange-coupled Mn(II) dimer reproduced the main features of the EPR spectra at both frequencies and yielded the zero-field splitting within the $S = 2$ manifold: $D_2 = -0.060 \pm 0.003$ cm^{-1}. The results of this study may aid in interpreting frozen solution EPR spectra of dinuclear manganese enzymes and model compounds. A novel signal at $g = 4.52$ was also observed, which exhibited a hyperfine splitting of 26 G. This signal may arise from the total spin 5/2 ground state of a Mn(II) trimer that forms from **1** in solution.

Acknowledgment. We thank Spiros Vellas of the Texas A&M Supercomputing Facility for assistance with DDPOWJHE. We thank the reviewers for helpful comments. Computer resources were provided by the Texas A&M Supercomputing Facility. This work was supported by the NSF (CAREER award to V.J.D., Grant CHE-8912763 for Texas A&M EPR facilities) and the Robert A. Welch Foundation. V.J.D. is a Cottrell Scholar of the Research Corporation.

Supporting Information Available: Full Q-band variable-temperature EPR spectra of **1** in a toluene solution, Q-band EPR spectra showing the changes in the intensities of the peaks during a serial dilution of **1** in toluene, comparison of the low-temperature (6 K) EPR spectra at both the Q-band and X-band to simulations of the $S = 1$ state of **1**, and comparison of the low-temperature EPR spectra to simulations of the $S = 2$ state of **1** using $D_2 = -0.060$ cm^{-1}. This material is available free of charge via the Internet at http://pubs.acs.org.

IC0000247